



## 1 Sensitivity of tropical woodland savannas to El Niño droughts

2 Simone Matias Reis<sup>1,2,3\*</sup>, Yadvinder Malhi<sup>1</sup>, Ben Hur Marimon Junior<sup>2</sup>, Beatriz Schwantes  
3 Marimon<sup>2</sup>, Huanyuan Zhang-Zheng<sup>1</sup>, Renata Freitag<sup>2</sup>, Cécile A. J. Girardin<sup>1</sup>, Edmar Almeida de  
4 Oliveira<sup>2</sup>, Karine da Silva Peixoto<sup>2</sup>, Luciana Januário de Souza<sup>2</sup>, Ediméia Laura Souza da Silva<sup>2</sup>,  
5 Eduarda Bernardes Santos<sup>2</sup>, Kamila Parreira da Silva<sup>2</sup>, Maély Dállet Alves Gonçalves<sup>2</sup>, Cecilia  
6 A. L. Dahlsjö<sup>1</sup>, Oliver Lawrence Phillips<sup>4</sup>, Imma Oliveras Menor<sup>1,5</sup>

7

8 <sup>1</sup>School of Geography and the Environment, Environmental Change Institute, University of  
9 Oxford, Oxford, UK

10 <sup>2</sup>Laboratório de Ecologia Vegetal/Programa de Pós-graduação em Ecologia e Conservação,  
11 Universidade do Estado de Mato Grosso, Nova Xavantina, BR

12 <sup>3</sup>Centro de Ciências Biológicas, Universidade Federal do Acre, Rio Branco, BR

13 <sup>4</sup>School of Geography, University of Leeds, Leeds, UK

14 <sup>5</sup>AMAP (Botanique et Modélisation de l'Architecture des Plantes et des Végétations), Université  
15 de Montpellier, CIRAD, CNRS, INRAE, IRD, Montpellier, France

16 Correspondence to: Simone Matias Reis (simonematiasreis@gmail.com)

17

### 18 Abstract

19 The 2015-2016 El Niño event led to one of the most intense and hottest droughts for many tropical  
20 forests, profoundly impacting forest productivity. However, we know little about how this event  
21 affected the Cerrado, the largest savanna in South America. Here we report 5 years of productivity  
22 of the dominant vegetation types in Cerrado, savanna (*cerrado*) and transitional forest-savanna  
23 (*cerradão*), continuously tracked before, during, and after the El Niño. We carried out intensive  
24 monitoring between 2014 and 2019 of the productivity of key vegetation components (stems,  
25 leaves, roots). Before the El Niño total productivity was ~25% higher in the *cerradão* compared  
26 to the *cerrado*. However, *cerradão* productivity declined strongly by 29% during the El Niño event.  
27 The most impacted component was stem productivity, reducing by 58%. By contrast, *cerrado*  
28 productivity varied little over the years, and while the most affected component was fine roots,  
29 declining by 38% during the event, fine root productivity recovered soon after the El Niño. The  
30 two vegetation types also showed contrasting patterns in the allocation of productivity to canopy,  
31 wood, and fine-root production. Our findings demonstrate that *cerradão* can show low resistance  
32 and resilience to climatic disturbances due to the slow recovery of productivity. This suggests that  
33 the transitional Amazon-Cerrado ecosystems between South America's largest biomes may be  
34 particularly vulnerable to drought enhanced by climate change.

35 **Keywords:** 2015-2016 El Niño, productivity, productivity allocation, climate events, *cerradão*,  
36 *cerrado*.

37

### 38 1 Introduction

39 The 2015-2016 El Niño event led to one of the most intense droughts of the last century as well  
40 as record maximum temperatures, coming on top of decades of long-term warming (Jiménez-



41 Muñoz et al., 2016; Liu et al., 2017). The 2015-16 climate anomaly affected most of the tropics  
42 but was especially potent in Amazonia (Gloor et al., 2018). Intense droughts can increase tree  
43 mortality and affect the carbon sequestration capacity of forests as shown by long-term ground-  
44 based monitoring (e.g., Phillips et al., 2009; Feldpausch et al., 2016; Rifai et al., 2018; Bennett et  
45 al., 2023). Satellite-based analyses also reveal the impacts of climate anomalies on carbon  
46 dynamics (Palmer et al., 2018; Fan et al., 2019), providing a synoptic view of ecosystem  
47 productivity. However, we still lack ground-based, tree-level measurements of net primary  
48 productivity (NPP) through extreme tropical climate events, hindering our understanding of key  
49 aspects of the vegetation carbon cycle response, such as recovery following drought events, and  
50 NPP allocation. Measuring these ecosystem responses directly is helped by tracking long-term  
51 forest dynamics in permanent plots but especially requires high-fidelity process-based  
52 measurements sustained over time. These are exceptionally challenging to make and require  
53 long-term dedication to measurements before, during, and after major climate events like the  
54 2015-16 El Niño. We know especially little about how the productivity of savanna ecosystems is  
55 affected by El Niño events, especially in the extensive Amazonia-Cerrado transition in South  
56 America.

57         The Amazonia-Cerrado transitional region contains a mixture of Amazonia and Cerrado  
58 species, making the species composition of this region unique and diverse (Ratter et al., 1973;  
59 Marimon et al., 2006; Morandi et al., 2016). Despite its ecological importance, this region has  
60 been greatly impacted by deforestation (~41% between 1984 and 2014) so that today only  
61 fragments of native vegetation remain (e.g., Marques et al., 2020). In recent decades, the  
62 remaining vegetation has been affected by increasing temperatures, frequent wildfires, extreme  
63 drought events, and the long-term lengthening of the dry season (e.g., Reis et al., 2018; Silvério  
64 et al., 2019; Nogueira et al., 2019; Matricardi et al., 2020; Araújo et al., 2021a). Deforestation,  
65 together with increases in temperature and reduction in precipitation during El Niño events,  
66 increases wildfire occurrence and carbon emissions, reducing the capacity of the vegetation to  
67 act as a carbon sink (Covey et al., 2021; Gatti et al., 2021). As the Amazonia-Cerrado transition  
68 is the driest, warmest, and most fragmented region in the Amazon basin (e.g., Matricardi et al.,  
69 2020; Marques et al., 2020; Covey et al., 2021; Reis et al., 2022) it is especially vital to understand  
70 better how climate change and extreme climate events impact carbon dynamics.

71         This transition is composed naturally of a mosaic of vegetation, being the typical cerrado  
72 (referred to as *cerrado* hereafter) and woodland savanna (i.e., *cerradão*) the most common in the  
73 regions (Ratter et al., 1973; Marimon et al., 2006; Oliveras & Malhi, 2016). Despite co-existing in  
74 the same space, *cerrado* and *cerradão* vegetation formations show contrasting characteristics  
75 (Marimon-Junior & Haridasan, 2005; Marimon et al., 2006). The *cerradão* is a transitional forest-  
76 savanna characterized by closed canopy, understory formed by small shrubs and herbs, with few  
77 grasses, and average height of the tree stratum varying from 8 to 15 m, tree cover of 50 to 90%  
78 (Ribeiro & Walter, 2008, Oliveras & Malhi 2016), while *cerrado* is a savanna vegetation type with  
79 a discontinuous canopy, trees, and shrubs with grass understorey, and a low average height of



80 just 3 to 6 m, with tree cover of 20 to 50% (Marimon-Junior & Haridasan, 2005; Ribeiro & Walter,  
81 2008).

82 In the *cerrado*, most species are deciduous, fully shedding their leaves in the dry season,  
83 while most *cerradão* species are brevi-deciduous. Although the dominant species of both  
84 vegetation types show strong stomatal efficiency (Jancoski et al., 2022), trees in the *cerrado* have  
85 smaller stomata and higher trichome density than individuals occurring in the *cerradão*,  
86 anatomical features that help the leaves minimise their water loss (Araújo et al., 2021b; Araújo et  
87 al., 2023). Furthermore, for species that co-occur in both *cerrado* and *cerradão*, individuals in  
88 *cerrado* lose their leaves earlier than *cerradão* in the dry season. The early loss of leaves in the  
89 *cerrado* means that the photosynthetic apparatus is not harmed during the driest and hottest  
90 period of the year. In the *cerradão*, individuals take longer to lose their leaves, which makes them  
91 more sensitive to changes in temperature increases, both current and projected (Araújo et al.,  
92 2021b). *Cerradão* trees are taller than *cerrado* trees, this characteristic may offer *cerradão* greater  
93 sensitivity to drought, since taller trees have wider xylem vessels (Araújo et al., *under review*).  
94 These characteristics (e.g., larger stomata and greater maximum stomatal pore opening) may  
95 give the *cerradão* greater sensitivity to disturbances generated by climatic anomalies, such as the  
96 2015-2016 El Niño.

97 Here, by setting up and sustaining intensive, long-term monitoring plots that experience  
98 a similar climate at *cerradão* and *cerrado*, we aimed to quantify and compare the effect of the  
99 2015/2016 El Niño on the carbon cycle (productivity and allocation) of these two vegetation types.  
100 Our guiding questions are: 1) Does productivity and allocation differ between *cerradão* and  
101 *cerrado*? 2) How did the 2015-2016 El Niño affect productivity and allocation in the *cerradão* and  
102 *cerrado*? 3) Did the *cerradão* and *cerrado* regain productivity after the El Niño? 4) What are the  
103 trade-offs in resource allocation between canopy, wood and fine roots during drought in the two  
104 vegetation types?

105

## 106 **2 Materials and Methods**

### 107 **2.1 Study sites**

108 We conducted this study in two long-term plots in *cerradão* (transitional forest-savanna – NXV-  
109 02; Forestplots code) and *cerrado* (*typical cerrado* – savanna – NXV-01) located in the Bacaba  
110 Municipal Park, in Nova Xavantina, Mato Grosso State, Central Brazil. The park covers  
111 approximately 500 ha in the transition zone between the Cerrado (Brazilian savanna) and  
112 Amazonia. Since the two plots are about 300m apart, they experience very similar climates, which  
113 corresponds to the *Aw* (tropical with dry winters) type in Köppen's classification system (Alvares  
114 et al., 2013). As measured by station #83319 of the Brazilian National Institute of Meteorology  
115 (INMET), the mean monthly temperature is 24.8 °C, the total annual precipitation is 1440 mm  
116 (Peixoto et al., 2017), and the average altitude of the park is ~ 250 m (Marimon Junior &  
117 Haridasan, 2005).

118 The plots were established in 2002 (Marimon Junior & Haridasan, 2005) and have been  
119 re-censused multiple times. Since 2010, these have been part of the PELD (Cerrado-Amazonia



120 Forest Transition: ecological and socio-environmental bases for Conservation), RAINFOR  
121 (Amazonia Forest Inventory Network; ForestPlots.net et al., 2021) and ForestPlots.net  
122 collaborations, and since 2014, part of GEM (Global Ecosystems Monitoring network; Malhi et al.,  
123 2021). The plots have facilitated multiple studies, such as soil, composition and diversity of  
124 species, biomass, and tree dynamics (e.g., Marimon Junior & Haridasan, 2005; Marimon et al.,  
125 2014). Partial data on carbon cycling have previously been published for the *cerradão* plot, on  
126 litterfall, soil efflux and carbon stocks at fine roots, litter layer, and stem (Peixoto et al., 2017;  
127 Peixoto et al., 2018). Here we provide the first comprehensive description of the carbon cycling  
128 in both plots as well as an extended time series that provides insight into the aftermath of  
129 2015/2016 El Niño event.

130 The plots have not been burned since 2008. The *cerradão* plot is a transitional forest-  
131 savanna characterized by the overlap of savanna and forest species, a closed canopy, and with  
132 dominant species (notably *Hirtella glandulosa* Spreng. and *Tachigali vulgaris* L.G. Silva & H.C.  
133 Lima). This type of *cerradão* was recognised by Ratter et al. (1973) as *Hirtella glandulosa*  
134 *cerradão*. Trees and shrubs with grass understorey and open canopy characterize the *cerrado*.  
135 Here the two dominant tree species are *Qualea parviflora* Mart. and *Davilla elliptica* A.St.-Hil.  
136 (Marimon Junior & Haridasan, 2005; Marimon et al., 2014). The vegetation of the *cerrado* is  
137 becoming denser and there are not many grasses present (Morandi et al., 2015), possibly due to  
138 fire exclusion.

139 The soil is similar across the plots – sandy loams of the yellow latosol type, acidic (pH <  
140 5.0) and dystrophic ( $\text{Ca}^{2+} \sim 0.4 \text{ cmol}_c \text{ kg}^{-1}$ ), with high levels of exchangeable aluminium ( $\text{Al}^{3+} >$   
141  $1.3 \text{ cmol}_c \text{ kg}^{-1}$ ) – however, the *cerradão* soil presents higher percentages of clay and potential  
142 water holding capacity than the *cerrado* (Marimon Junior & Haridasan, 2005). These differences  
143 in soil texture may explain the different vegetation formations in these two closely adjacent sites.  
144 The average height of the trees in *cerrado* is 3.7 m, and a basal area of  $\sim 14.9 \text{ m}^2 \text{ ha}^{-1}$ . For the  
145 *cerradão*, the average tree height is 6.4 m and basal area of  $\sim 21.4 \text{ m}^2 \text{ ha}^{-1}$  (Marimon Junior &  
146 Haridasan, 2005). The species number was 77 in both and the number of trees similar (*cerrado*  
147 = 1890 and *cerradão* = 1884) (Marimon Junior & Haridasan, 2005).

148

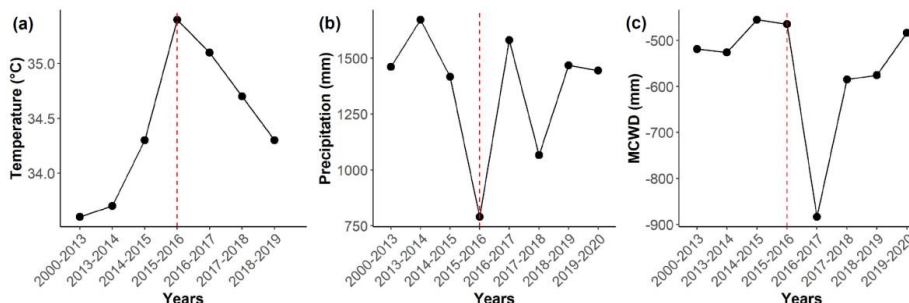
## 149 **2.2 Site climate and the El Niño 2015/2016 event**

150 We used the climate variables – air temperature, relative air humidity, and precipitation – in time  
151 series from a Meteorological Station (World Weather Station 83319), about 800 m from the plots.  
152 We calculated the maximum climatological water deficit (MCWD), a climatological measure of  
153 tropical forest water stress (see Aragão et al., 2007). To calculate MCWD, we considered a  
154 standardized evapotranspiration (ET) value for wet season tropical forests of 100 mm month<sup>-1</sup>  
155 (Aragão et al., 2007).

156 The seasonality of the plots is marked by two well-defined seasons – cooler-dry (April to  
157 September) and hot-rainy (October to March). We defined the twelve months from May 2015 to  
158 April 2016 as the climate of the 2015-2016 El Niño Southern Oscillation event based on Liu et al.  
159 (2017). During the El Niño, the plots experienced record mean and mean monthly maximum



160 annual temperatures (26.0 °C and 35.4 °C) and record low total annual precipitation (790.2 mm),  
 161 and in September 2016, record low annual MCWD (-883.7 mm) (Fig. 1; Table S1).  
 162



163  
 164 **Fig. 1. Climate variables** between 2000 and 2020 for *cerrado* and *cerradão*. We should (a)  
 165 temperature (°C), (b) precipitation (mm/year) and (c) maximum climatological water deficit  
 166 (MCWD, mm in a rolling year) with the 1st month of the dry season (May) representing the  
 167 beginning of each year's climatic calendar. The temperature indicates the average maximum  
 168 monthly temperatures. The dashed red line indicates the El Niño periods. Climatic data are from  
 169 meteorological station #83319 of the Brazilian National Institute of Meteorology (INMET). See  
 170 Table S1 for data.  
 171

172 **2.3 Field methods**

173 We followed the GEM protocol manual (Marthews et al., 2014; Malhi et al., 2021) to collect the  
 174 data for this study. We measured the main components of NPP: canopy (leaves, twigs,  
 175 reproductive parts, and others), wood (stems and branches), and fine roots (see Table 1).  
 176

177 **Table 1.** Field methods for intensive monitoring of NPP components from *cerradão* (NXV-02) and  
 178 *cerrado* (NXV-01) plots in the transition zone between Amazonia and Cerrado. See also the  
 179 RAINFOR-GEM manual (Marthews et al., 2014). nc= no collected.

Component	Description	Sampling period	Sampling interval
<b>Above-ground net primary productivity (<i>NPP<sub>AG</sub></i>) and biomass</b>			
Aboveground coarse wood net primary productivity ( <i>NPP<sub>stem</sub></i> ) and Stem biomass	<b>Forest inventory</b> or plot census were done in the years listed. The default measurement point was set at 30cm ( <i>DAS<sub>30cm</sub></i> ) above soil surface, instead of a typical forest diameter at breast height at 1.3m. All trees ≥ 5 cm <i>DAS<sub>30cm</sub></i> were censused, based on which, we calculated mortality and recruitment rate of new trees. <b>Stem biomass</b> for each tree was calculated. The sum of all alive trees in each census is termed stem biomass. As we have noticed trees stem shrinking, we calculate stem NPP as the change of alive trees biomass between two censuses, where dead and new recruit trees are excluded but shrinking trees are included. We have also presented 'Stem Diameter growth' which excludes shrinking trees, dead trees and new recruit trees. In 2014, five 10 m x 10 m subplots were established to census small trees (≤ 5 cm <i>DAS<sub>30cm</sub></i> ) to estimate the biomass fraction of smaller trees and data scaled up to 1 ha. Standing dead trees biomass is measured using similar method and not counted in Stem Biomass.	2013 – 2021 (NXV-01) 2013 – 2020 (NXV-02)	2013, 2015, 2018 and 2021 (NXV-01) 2013, 2015, 2017 and 2020 (NXV-02)




---

	<p>Biomass of each stem was calculated using Rezende et al. (2006) specific allometric equation for the Cerrado: <math>C = 0.24564 + 0.01456 \cdot (D/10)^2 \cdot H</math> where C is aboveground Carbon stocks (kg), D is the diameter (30 cm above the soil), and H is the height (m). The authors assumed that dry stem biomass is 50% carbon. Systematic uncertainty of +25% was assigned to values for error propagation. Errors calculated as the sampling error associated with variation between the transects.</p>		
<p>Branch turnover net primary productivity (<math>NPP_{\text{branch turnover}}</math>)</p>	<p>Branchfall &gt; 2 cm diameter (excluding that associated with dead trees) surveyed within four 1 m x 100 m transects; small branches were cut to include only the transect-crossing component, removed, and weighed. Larger branches had their dimensions taken (diameter at three points), and assigned a wood density value according to decomposition class (Harmon et al., 1995). Biomass of each branch was calculated. The first collection of branchfall in 2014 lead to 'woody debris biomass', which accounts for necromass in the ground litter layer. 'Woody debris biomass' is not included in above nor belowground biomass. The biomass of branch has been implicitly included in <math>NPP_{\text{stem}}</math>. Branchfall was then collected from the same transects every 3 months which lead to <math>NPP_{\text{branch turnover}}</math></p>	2014 – 2019	Every 3 months
<p>Litterfall net primary productivity (<math>NPP_{\text{litterfall}}</math>)</p>	<p>Litterfall production of dead organic material (&lt; 2 cm diameter) calculated by collecting litterfall in 0.2827 m<sup>2</sup> circular collectors placed at 1 m above the ground at the center of each of the 25 subplots in each plot. Litter separated into leaves, twigs, reproductive parts (flowers, fruits, and seeds), and unidentifiable. <math>NPP_{\text{litterfall}}</math> calculated as follows: <math>NPP_{\text{litterfall}} = NPP_{\text{canopy}} - \text{Loss to Leaf Herbivory}</math>. Litterfall separated into different components, oven-dried at 65°C to constant mass, and weighed. Litter estimated to be 49.2% carbon, based on mean Amazonia values (S. Patiño, unpublished analysis). Errors calculated as the sampling error associated with variation between the litter traps.</p>	Jan 2014 – Dec 2019	Every 14 days
<p>Leaf Area Index (LAI) and Leaf biomass</p>	<p>Hemispherical photos taken with a digital camera (Nikon OP 10mm) and hemispherical lens (Nikon 10mm fisheye lens) near the center of each of the 25 subplots in each plot at a standard height of 1 m and during overcast conditions. LAI estimated from these images using Hemisfer software (licensed version 2.12; <a href="http://www.wsl.ch/dienstleistungen/produkte/software/hemisfer/index_EN">http://www.wsl.ch/dienstleistungen/produkte/software/hemisfer/index_EN</a>). LAI estimated from hemispherical photos using the standard Li-Cor LAI-2000 method, based on the Miller (1967) equations, and correcting for non-linearity and slope effects (Schleppi et al., 2007) and canopy clumping (Chen &amp; Cihlar, 1995). Thresholds were set to detect separately for each ring (6 rings) according to Nobis &amp; Hunziker (2005). Errors calculated as the sampling error through variation among subplots. Leaf biomass calculated as leaf area index (LAI)/specific leaf area (SLA), where LAI is the plot mean over the study period, and SLA is the basal area-weighted plot mean</p>	Jun 2015 – Jan 2020	Every 3 months

---



	over the study period. We used the SLA value of March 2014 (Neyret et al., 2016).		
Loss to leaf herbivory ( $NPP_{\text{herbivory}}$ )	Estimated based on Neyret et al. (2016)'s observation that the loss to herbivory was 3.11% in NXV-01 and 4.43% in NXV-02. The data collection was conducted between March and May 2014. Each leaf's fractional herbivory ( $H$ ) was calculated as $H = (A_{\text{nh}} - A_h) / A_{\text{nh}}$ . Where $A_h$ is the area of each leaf, including the damage incurred by herbivory, and $A_{\text{nh}}$ is the leaf area prior to herbivory (Neyret et al., 2016). The average value of $H$ of all leaves collected per litterfall trap was derived, and plot-level means were calculated. Systematic uncertainty of $\pm 50\%$ assigned to values for error propagation.	nc	nc
<b>Below-ground net primary productivity (<math>NPP_{\text{BG}}</math>)</b>			
Coarse root net primary productivity ( $NPP_{\text{coarse root}}$ )	Root biomass estimated based on Miranda et al. (2014) that is specific for the vegetation types of Cerrado. Based on this study, the Root(belowground): shoot ratio (aboveground) biomass is 1.37 to <i>cerrado</i> and 0.22 to <i>cerradão</i> . Systematic uncertainty of $\pm 20\%$ assigned to values for error propagation. We used these ratios, 1.37 (at NXV-01) and 0.22 (at NXV-02) to derive $NPP_{\text{coarse root}}$ from $NPP_{\text{stem}}$	nc	nc
Fine root net primary productivity ( $NPP_{\text{fine root}}$ ) and fine root biomass	In each plot, sixteen ingrowth cores (mesh cages 12 cm diameter, to 30 cm depth) were installed. Roots were manually removed from the soil samples in four 10 min time steps, according to a method that corrects for underestimation of biomass of hard-to-extract roots (Metcalf et al., 2007) and used to predict root extraction beyond 40 min (up to 120 min); typically, there was an additional 33% correction factor for fine roots not collected within 40 min. Correction for fine roots productivity below 30 cm depth (Galbraith et al., 2013) increased the value by 39%. Errors were calculated as the sampling error associated with variation between the sampling points.  Root-free soil was then re-inserted into the ingrowth core. Collected roots were thoroughly rinsed, oven-dried at 65°C to constant mass, and weighed. This process was repeated for each measurement thereafter. <b>Fine root biomass</b> was calculated from harvested fine roots during the first installation of ingrowth. The subsequent fine root collection from the ingrowth cores lead to $NPP_{\text{fine root}}$	Sep 2014 – Feb 2020	Every 3 months

180

181

182 **2.4 NPP calculation**

183 We measured the NPP in the two plots between 2014 and 2020 (Table 1). We calculated all major  
184 components of NPP using the following equations:

185  $NPP_{\text{total}} = NPP_{\text{coarse root}} + NPP_{\text{fine root}} + NPP_{\text{stem}} + NPP_{\text{branch}} + NPP_{\text{litter fall}} + NPP_{\text{herbivory}}$  (1)

186  $NPP_{\text{canopy}} = NPP_{\text{litter fall}} + NPP_{\text{herbivory}}$  (2)

187  $NPP_{\text{woody}} = NPP_{\text{coarse root}} + NPP_{\text{stem}} + NPP_{\text{branch turnover}}$  (3)

188  $NPP_{\text{root}} = NPP_{\text{fine root}}$  (4)





189  $NPP_{ACW} = NPP_{stem}$  (5)

190

191 Our calculations above neglect several small NPP terms, such as NPP lost as volatile  
192 organic emissions ( $NPP_{VOC}$ ), unmeasured litter trapped in the canopy, or litter dropped from  
193 understorey flora below the litter traps (1 m). However, in central Amazonia, Malhi et al. (2009)  
194 found  $NPP_{VOC}$  was a relatively minor NPP term ( $0.13 + 0.06 \text{ Mg C ha}^{-1} \text{ year}^{-1}$ ). For belowground  
195 NPP, we do not include root exudates and mycorrhizae that account for  $< 2 \text{ Mg C ha}^{-1} \text{ year}^{-1}$ ,  
196 representing a modest part of the carbon fluxes (Malhi et al., 2017). Thus, we focus on the canopy,  
197 wood, and fine roots productivity, which account for over 85% of NPP (See Riutta et al., 2018 and  
198 their references).

199 We calculated the relative allocation to the main NPP components (woody, canopy, and  
200 fine roots NPP) for leaves, fine roots, and stem following the equations:

201  $Allocation_x = (NPP_x * 100)/NPP_{total}$  (6)

202

### 203 **2.5 Calculation of measurements uncertainty**

204 Estimation of measurements uncertainty for each NPP component is explained in details in Table  
205 1. For components that are not directly measured, for example  $NPP_{total}$  as a sum of several  
206 components, we combine relevant error by error propagation with standard quadrature rules  
207 (Hughes & Hase, 2010; Malhi et al., 2015). During the above process, we also assigned significant  
208 systematic errors to capture uncertainties related to sampling methodology or scaling approaches  
209 (see Table 1); these factors were consistent with those applied in similar previous studies (Malhi  
210 et al., 2009, 2015; 2017; Girardin et al., 2010; Galbraith et al., 2013).

211

### 212 **2.6 Data analyses**

213 Our analyses were focused on comparing NPP among the years (2014 to 2019) – comprising the  
214 periods before, during, and after the El Niño 2015/2016 events – in *cerrado* and *cerradão*. We  
215 compared the stem and canopy biomass of the two vegetation types over time using repeated  
216 two-way analysis of variance (ANOVA-two way). We used Tukey's post hoc test to compare the  
217 different years in each plot. We used the same analysis to compare productivity and carbon  
218 allocation across different compartments. In cases where the residuals violated the ANOVA  
219 assumptions, we used Friedman's non-parametric analysis. We performed all analyses in the R  
220 environment and adopted a significance level of 0.05. To improve the accessibility of colour  
221 figures with COLORBREW 2.0.

222

## 223 **3 Results**

### 224 **3.1 Net primary productivity**

225 The net primary productivity (NPP) in the *cerradão* was ~ 30% higher compared to that of the  
226 *cerrado* prior to the occurrence of El Niño (*cerradão* =  $\sim 9.3 \pm 0.57 \text{ Mg C ha}^{-1} \text{ year}^{-1}$ ; *cerrado* =  
227  $\sim 6.5 \pm 1.12 \text{ Mg C ha}^{-1} \text{ year}^{-1}$  Fig. 2; Table S2). This is due to the greater productivity in the canopy  
228 and stem in the *cerradão* (Fig. 2; Table S2). During the El Niño, *cerradão* NPP decreased to



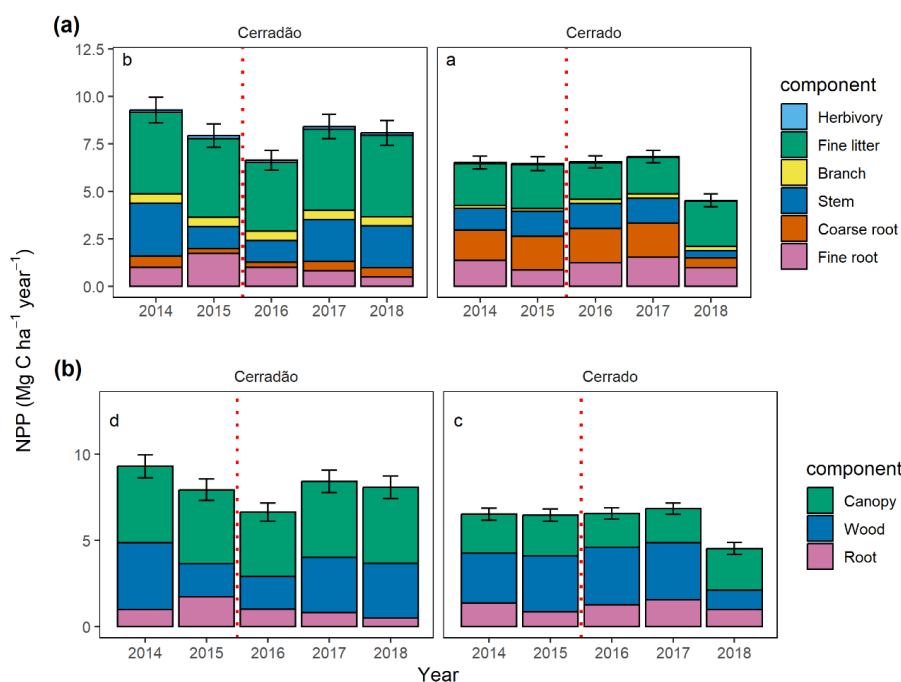


229  $6.6 \pm 0.6 \text{ Mg C ha}^{-1} \text{ year}^{-1}$  and became similar to the *cerrado* ( $6.6 \pm 1.3 \text{ Mg C ha}^{-1} \text{ year}^{-1}$ ; Fig. 2;  
230 Table S2).

231 *Cerradão* NPP was severely affected in 2016 during the El Niño event (-29%). In 2018 it  
232 was still 13% lower than pre-El Niño conditions (Fig. 2). Additionally, stem biomass declined  
233 significantly after El Niño ( $F = 19.3, p < 0.001$ ) and did not return to the values registered before  
234 the event (Fig. S1).

235 In the *cerrado*, NPP did not vary much before and during the El Niño. However, in 2018,  
236 productivity reduced by ~30%, due especially to the reduction in stem productivity. Despite this,  
237 stem biomass was not significantly influenced by El Niño and increased significantly between  
238 2013 and 2018 ( $F = 3.1; p < 0.05$ ), remaining stable until 2021 (Fig. S1).

239



240

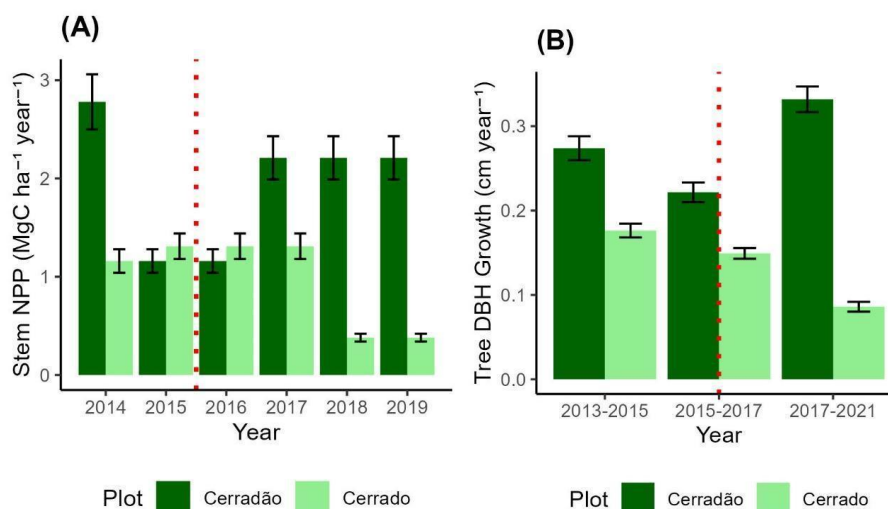
241 **Fig. 2.** Mean total annual net primary productivity (NPP) between 2014 and 2018 split into its  
242 components (a) and annual NPP allocation into the canopy, wood, and root components (b) at  
243 *cerrado* and *cerradão*. The branch data from *cerradão* was collected in 2014 and repeated in  
244 other years. The error bars represent the standard error for total NPP. The dashed red line  
245 indicates the El Niño periods.  
246

247

248 In the *cerradão*, the most affected component was stem net primary productivity (NPPs),  
249 which was reduced by 58% during and after El Niño ( $F = 15.6, p < 0.001$ ; Fig. 3A). In 2019 it was  
250 still -21% lower than pre-El Niño conditions. When we consider only those trees that were alive  
251 before El Niño and remained alive after the event, the *cerradão* reduced NPPs significantly during  
252 the event, but after the event, NPPs was greater than before the El Niño (Fig. 3B;  $F = 25.6, p <$



253 0.001). This is mainly due to two critical species for this transitional forest, *Hirtella glandulosa*  
 254 Spreng. and *Tachigali vulgaris* L.G.Silva & H.C.Lima, which contributed 22% and 17% to NPPs  
 255 after El Niño. Before El Niño, *T. vulgaris* was the species that most contributed to NPPs (26%).  
 256 In the *cerrado*, trees showed less diameter growth during and after the event (Fig. 3B;  $F= 109.7$ ,  
 257  $p< 0.001$ ). However, stem productivity was not affected during the event (Fig. 3A).  
 258



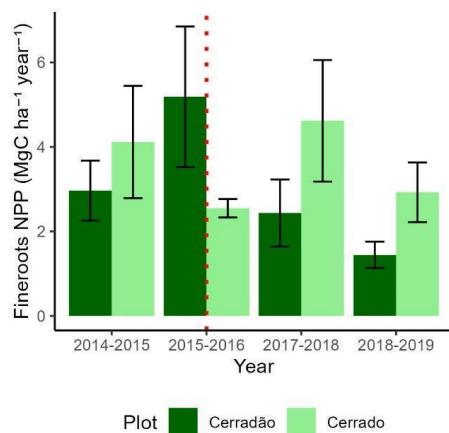
259

260 **Fig. 3.** Stem dynamics in *cerrado* (light green) and *cerradão* (dark green). (a) Stem net primary  
 261 productivity (NPP<sub>stem</sub>, MgC ha<sup>-1</sup> year<sup>-1</sup>) for stem larger than 5cm diameter. We note that there  
 262 are negative stem NPP values due to those trees that lose bark or water from the stem in the dry  
 263 periods, especially in *cerrado* after 2017. (b) The growth of tree diameter (measured at 30cm  
 264 above soil surface) (cm year<sup>-1</sup>), calculated as the increase in DAS between two censuses divided  
 265 by time. Only growth is included, in other words, trees with shrinking stems are excluded. The  
 266 dashed red line indicates the El Niño periods.  
 267

268

269 In the *cerradão*, fine root net primary productivity (NPP<sub>fr</sub>) production increased significantly  
 270 (+42%) during El Niño ( $F= 17.3$ ,  $p< 0.001$ ), but in later years productivity declined (Fig. 4). The  
 271 *cerrado* presented the opposite pattern observed in the *cerradão*. NPP<sub>fr</sub> reduced by 38% during  
 272 the event ( $F= 5.6$ ,  $p= 0.001$ ; Figs. 2 and 4). However, the NPP<sub>fr</sub> of this component re-established  
 273 itself soon after El Niño, but experienced a decline of ~ 38% in 2018.  
 274

274



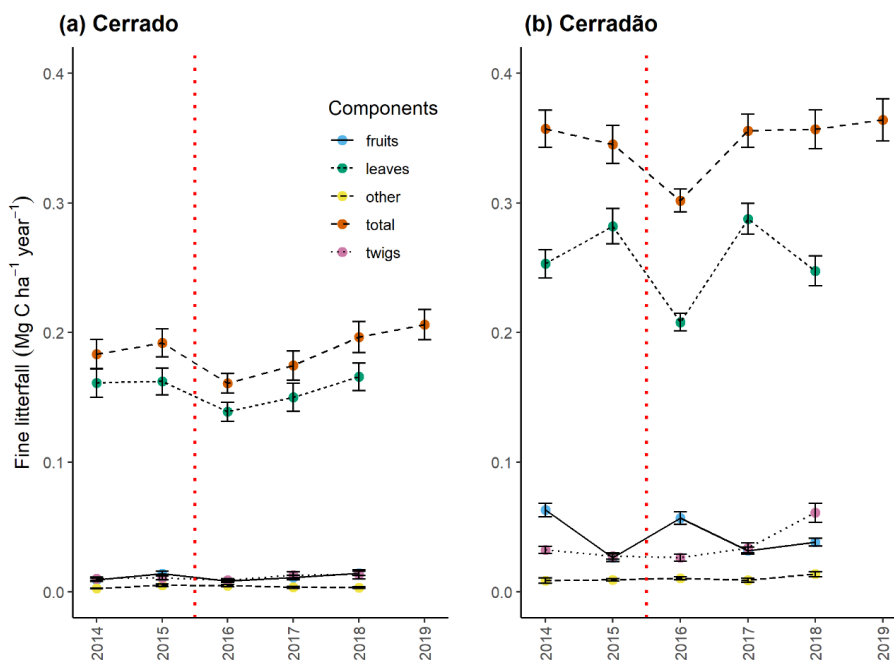
275

276 **Fig. 4.** Fine root net primary productivity (NPPfr) for *cerrado* (light green) and *cerradão* (dark  
277 green) between September 2014 and August 2019. The error bars represent the standard error.  
278 The dashed red line indicates the El Niño periods.  
279

280

281 Canopy productivity was affected after the El Niño event in both *cerradão* ( $F=2.8$ ,  $p=0.01$ )  
282 and *cerrado* ( $F=6.7$ ,  $p<0.001$ ) (Fig. 5). However, the NPP of this component was re-established  
283 two years after the event. For the *cerradão*, it is worth highlighting the drop in fruit production after  
284 the event, which had not yet re-established itself two years after El Niño (Fig. 6). Furthermore,  
285 after El Niño, both plots show declining and then recovering LAI (Fig. S2). We also noted that  
286 following El Niño, the variability of LAI increased among subplots, potentially due to clearings  
287 emerging from heightened tree mortality. The average annual mortality rate increased during and  
288 after El Niño, especially in the *cerradão* (Fig. 6).

289

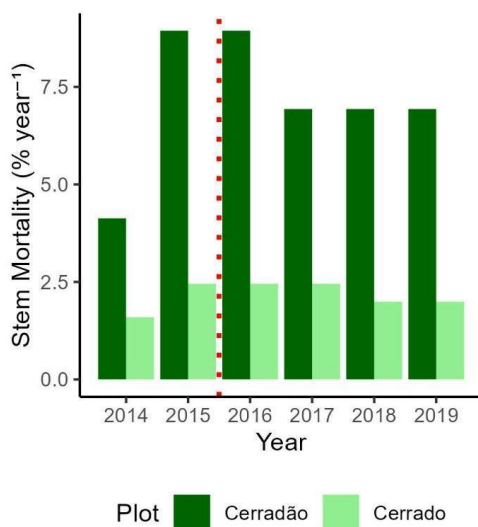


290

291 **Fig. 5.** Mean monthly productivity in canopy litterfall and its components for *cerrado* (a) and  
 292 *cerradão* (b) between 2014 and 2019: (fruits) flower, fruit, and seed fall; (leaves) leaf fall; (other)  
 293 not identified and (total) total canopy fine litterfall (as measured in litter traps); (twigs) twig fall (<  
 294 2 cm). The error bars represent the standard error. The dashed red line indicates the El Niño  
 295 periods.

296

297



298

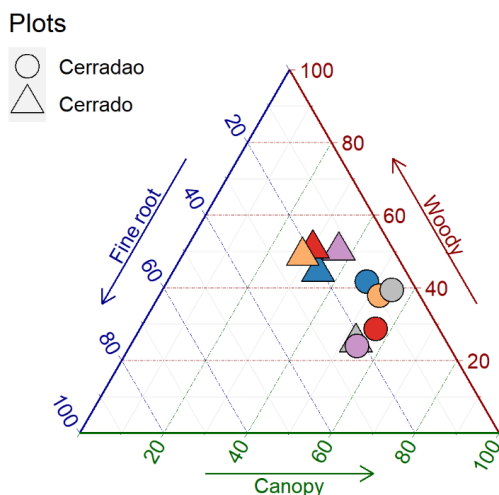


299 **Fig. 6.** Stem mortality, shown as the percentage of dead trees to the number of trees in the first  
 300 census divided by time. The dashed red line indicates the El Niño periods.  
 301

302

303 **3.2. Allocation between plots, components, and years**

304 In general, NPP allocation differed significantly between *cerradão* and *cerrado* plots (Fig. 7), but  
 305 this varies within the components ( $F= 41.7, p< 0.001$ ). The allocation to canopy was greater in  
 306 *cerradão* ( $53\pm 3\%$ ) than in *cerrado* ( $37\pm 10\%$ ). In contrast, allocation to woody and roots was  
 307 greater in the *cerrado* (woody=  $44\pm 11\%$ ; roots=  $19\pm 4\%$ ) than in the *cerradão* (woody=  $34\pm 8\%$ ;  
 308 roots=  $13\pm 6\%$ ). Over the studied time, the NPP allocation showed inter annual variation in *cerrado*  
 309 but no clear drought signal the main axis of interannual variation was a trade-off between canopy  
 310 investment and root allocation, with woody allocation remaining constant (Fig. 7). However, in  
 311 2018, ~ three years after El Niño, the allocation of canopy and wood changed drastically, showing  
 312 an opposite pattern to previous years. In the *cerradão*, there is a clear drought signal with  
 313 increased investment in fine roots during the drought, and reduced investment in woody growth;  
 314 canopy allocation remained fairly constant.  
 315



316

317 **Fig. 7.** Relative allocation (% of total) of net primary productivity (NPP) to canopy, woody, and  
 318 fine root NPP in *cerrado* and *cerradão*. 2014= blue, 2015= pink, 2016= red, 2017=orange and  
 319 2018= grey. Woody components include stem, coarse root and branch turnover; Fine root  
 320 includes fine root NPP only (no roots exudates); Canopy includes litterfall and herbivory  
 321

322

323

323 **4 Discussion**

324 *Cerradão* and *cerrado* showed contrasting responses to the 2015/2016 El Niño-associated  
 325 drought event. The *cerrado* proved to be more resistant and resilient, i.e., most of the parameters



326 assessed (e.g., stem carbon stock, canopy productivity) changed little during the event, and those  
327 that experienced a reduction soon re-established themselves (e.g., production of fine roots). In  
328 contrast, the *cerradão* showed lower resistance and resilience: stem carbon stock and mortality,  
329 productivity and allocation were affected during and after the El Niño event and even three years  
330 after, most of the parameters assessed were not similar to those observed before the event. Our  
331 findings demonstrate the high sensitivity of the *cerradão* to extreme drought events.

332 The productivity found in our *cerradão* ( $9.3 \pm 0.57$ ) was similar to that observed in transitional  
333 forests in Africa (9.2 to 13.1; Moore et al., 2018), and some low-fertility humid forest sites in  
334 lowland Amazonia in Colombia and Brazil ( $-8.1$  to  $10.3$ ; Aragão et al., 2009; Girardin et al., 2010).  
335 It is markedly greater than observed in seven premontane and montane sites in Peru ( $-3.9$  to  $6.4$ ;  
336 Girardin et al., 2010) and lower than observed in lowland tropical forest plots in south-western  
337 Amazonia ( $15.1 \pm 0.8$  and  $14.2 \pm 1.0$ ; Malhi et al., 2015) and nutrient-rich soils forests ( $17.0 \pm 1.4$ ;  
338 Aragão et al., 2009). Nevertheless, the total productivity of *cerradão* was more affected ( $-29\%$ )  
339 than the Amazonia rainforest ( $-7.6\%$  to  $-8.5\%$ ) during the El Niño drought of 2015/2016 (Machado-  
340 Silva et al., 2021). Moreover, the reduction in stem productivity was much larger ( $-58\%$ ) than that  
341 estimated for tropical forests as a whole ( $-8.3\%$  in 1997/1998, and  $-9\%$  in 2015/2016 (Rifai et al.,  
342 2018). This demonstrates the high sensitivity of this vegetation to climate anomalies.

343 The higher mortality of *cerradão* may be related to the hydraulic characteristics of the main  
344 species, such as *Tachigali vulgaris*, a pioneer species with stomatal control tending to an  
345 anisohydric condition and, therefore, more susceptible to hydraulic failure (Jankoski et al., 2022).  
346 In addition, many species are brevi-deciduous, so the plants continue to photosynthesize even  
347 during water scarcity (e.g., Jancoski et al., 2022). Other factors, such as a lack of strategies to  
348 avoid water loss, may also contribute, like low trichome density in their leaves and smaller stomata  
349 (Araújo et al., 2021b). Another possible cause of the high mortality in the *cerradão* is the unusually  
350 intense winds that hit trees with xylem tissue already weakened by the effects of drought and heat  
351 due to the El Niño event (Reis et al., 2022). *Cerradão* trees are taller than *cerrado* trees, which  
352 makes them more susceptible to wind disturbances. Once broken, even just part of the crown,  
353 the tree is at greater risk of death (Reis et al., 2022).

354 Despite the high mortality, the trees that remained alive showed higher stem productivity  
355 than before the El Niño. This may be related to the greater opening of clearings, favouring carbon  
356 uptake and plant growth due to the greater availability of light, water and nutrients to the remaining  
357 trees. During the El Niño drought, a decline in the growth of *Tachigali vulgaris* trees was observed,  
358 leading to a shift in the primary contributor to stem productivity from *T. vulgaris* to *Hirtella*  
359 *glandulosa*. The role reversal of these two species can be explained by the high mortality and low  
360 growth rate of *T. vulgaris* during and after El Niño. *T. vulgaris* is considered a key species for  
361 *cerradão* due to its high biomass gain after disturbances such as fire (Reis et al., 2015; 2017),  
362 but it is sensitive to drought. The high sensitivity of *T. vulgaris* to drought events may be attributed  
363 to the increased xylem tension required to extract water from the soil, making it more prone to  
364 embolism (Jancoski et al., 2022). Consequently, this results in reduced growth and higher  
365 mortality compared to *H. glandulosa*. On the other hand, *H. glandulosa* proved to be more



366 resistant: it has high foliar trichome density, which works as a strategy to prevent water loss (e.g.  
367 Gianoli & González-Teuber, 2005; Araújo et al., 2021b). In the *cerrado*, we observed the opposite  
368 pattern; the productivity of trees that remained alive continued to decline after the event. In this  
369 vegetation type, plant mortality was low, and the surviving plants had to compete to stay alive,  
370 which may explain the lower productivity after El Niño. Furthermore, many trees in the *cerrado*  
371 shed their outer bark, which may have affected the diameter measurement and, consequently,  
372 the productivity of the stem. The loss of bark from *cerrado* plants, especially after fire and drought  
373 events, makes the measurement of trunk productivity inaccurate.

374 The high production of fine roots in *cerradão* during drought is probably a strategy to  
375 increase soil water uptake during the period of soil water scarcity (Metcalfe et al., 2008). However,  
376 this strategy on partially ameliorates drought risk, as tree mortality was high even with a high  
377 investment in fine roots. The *cerrado*, on the other hand, showed the opposite strategy, investing  
378 less in fine roots during the event. However, shortly afterwards, the productivity of this component  
379 was similar to that observed before El Niño. Lowland *terra firme* have less root growth during the  
380 dry season but had greater specific root length and surface area where soil moisture was depleted  
381 (Metcalfe et al., 2008), and the *cerradão* presented a strategy similar to these Amazonia forests,  
382 but not the *cerrado*.

383 Both *cerrado* and *cerradão* adopted the strategy of losing more leaves during El Niño. It is  
384 well known that during periods of water stress in the soil, plants lose their leaves as a strategy to  
385 avoid water loss and consequent mortality (e.g., Brando et al., 2008). This strategy can also have  
386 nutrient cycling benefits: the nutrients released to the litter layer and soil after leaf drop and can  
387 later be reabsorbed by the plants when they re-establish leaf growth after a high stress period  
388 (e.g., Oliveira et al., 2017). The high leaf loss during El Niño may have contributed to lower  
389 photosynthetic activity of plants (e.g., Luo et al., 2018; Kaewthongrach et al., 2020), consequently  
390 affecting carbon accumulation.

391 The canopy-wood-fine root trade-offs identified here are different from those reported by  
392 Doughty et al. (2014) for a somewhat similar Amazonian forest-dry forest transition in Bolivia, with  
393 similar rainfall but more fertile soils. There, the site with better water availability (related to soil  
394 properties) hosted an Amazonian forest which showed wood-canopy trade-offs during drought.  
395 The drier site hosted *chiquitano* dry forest with wood-fine root trade-offs during drought. Our  
396 *cerradão* site shows similar wood-fine root trade-offs to the *chiquitano* forest, whereas our *cerrado*  
397 site shows a different canopy-fine root trade off. One possibility is that these shifting trade-off  
398 strategies reflect points on an aridity continuum from sub-humid Amazonian forest (wood-canopy  
399 trade-off) through transitional or seasonally dry forests (wood-fine root trade-off) through to  
400 savanna (wood-canopy trade-off). Alternatively, the differences in soil fertility may play a role,  
401 changing the costs and advantages of investment in fine-root production.

402

403

404

405





406 **5 Conclusions**

407 *Cerradão* is a vital transitional vegetation type at the Amazon-Cerrado ecotone, as it is in contact  
408 with the two main Brazilian biomes, Cerrado and Amazonia. However, this vegetation type  
409 appears to be susceptible to climatic events (*present study*), wildfires (Reis et al., 2015; 2017)  
410 and wind storms (Reis et al., 2022). One of the most frequent species in *cerradão* (*T. vulgaris*),  
411 that is especially important for carbon uptake, proved to be very sensitive to the climatic event.  
412 Thus, if these extreme drought events continue to become more frequent and intense, *cerradão*  
413 may release more carbon than absorbs, as observed here. In addition, the *cerradão* serves as a  
414 connection between the savanna and the forest, acting as a kind of buffer-barrier for the Amazonia  
415 to the effects of environmental stressors along its contact with the *cerrado*. Our results suggest  
416 that the more frequent occurrence of El Niño events can break this natural barrier, creating  
417 conditions for the progressive degradation of the forest along the edges.

418

419 **Author Contributions:** S.M.R. wrote the manuscript with input from all authors (Y.M., B.H.M.Jr.,  
420 R.F., B.S.M., H.Z., C.A.J.G., E.A.O., K.S.P., L.J.S., E.L.S., E.B.S., K.P.S., M.D.A.G., C.A.L.D.,  
421 O.L.P. and I.O.M.); Y.M., B.H.M.Jr. and I.O.M. were involved in planning and supervised the work;  
422 S.M.R., R.F., E.A.O., K.S.P., L.J.S., E.L.S., E.B.S., K.P.S. and M.D.A.G. performed the field  
423 measurements; S.M.R., H.Z., and C.A.J.G. performed the analyses and made the figures. All  
424 authors discussed the results and contributed to the final manuscript.

425

426 **Data availability statement:** The data are available at Dryad:  
427 <https://doi.org/10.5061/dryad.rjdfn2zhw> (Reis, 2023).

428

429 **Funding statement:** National Council for Scientific and Technological Development (CNPq) -  
430 financial support of the projects PELD “Cerrado-Amazonia Transition: ecological and socio-  
431 environmental bases for Conservation” (stages II, III and IV) - 403725/2012-7, 441244/2016-5  
432 and 441572/2020-0, PPBIO “Phytogeography of the Amazon-Cerrado Transition Zone”  
433 (457602/2012-0) and FAPEMAT (164131/2013 and 0589267/2016). S.M.R. was funded by a  
434 postdoctoral Fellowship from NERC and FAPESP (BIO-RED 2015/50517-5). This paper is a  
435 product of the Global Ecosystems Monitoring (GEM) Network, which was supported by an ERC  
436 Advanced Investigator Award to YM.

437

438 **Acknowledgements:** We thank the team of the Laboratório de Ecologia Vegetal - Plant Ecology  
439 Laboratory at the UNEMAT (Universidade do Estado de Mato Grosso) campus in Nova  
440 Xavantina, especially to Carla Heloísa Luz de Oliveira, Camila Borges, Erica Prestes Ferreira,  
441 Luiz Macedo Schuwaab Júnior, Erika Camila Oliveira, Izabel Amorim, Eder Carvalho das Neves,  
442 Kelen Alves Cavalheiro and Poliana Alves Cavalheiro for help collecting field data. We also thank  
443 the National Council for Scientific and Technological Development (CNPq) for financial support  
444 of the projects PELD “Cerrado-Amazonia Transition: ecological and socio-environmental bases  
445 for Conservation” (stages II, III and IV) - 403725/2012-7, 441244/2016-5 and 441572/2020-0,  
446 PPBIO “Phytogeography of the Amazon-Cerrado Transition Zone” (457602/2012-0) and



447 FAPEMAT (164131/2013 and 0589267/2016). We also thank CNPq for research productivity  
448 grants PQ1 to B.S. Marimon and B.H. Marimon Junior. S.M.R. was funded by a postdoctoral  
449 Fellowship from NERC and FAPESP (BIO-RED 2015/50517-5). This paper is a product of the  
450 Global Ecosystems Monitoring (GEM) Network, which was supported by an ERC Advanced  
451 Investigator Award to YM.

452

#### 453 **Competing interests**

454 The contact author has declared that none of the authors has any competing interests.

455

#### 456 **References**

- 457 Alvares, C. A., Stape, J. L., Sentelhas, P. C., Gonçalves, J. D. M., & Sparovek, G. (2013).  
458 Köppen's climate classification map for Brazil. *Meteorologische Zeitschrift*, 22(6), 711-728.
- 459 Aragão, L. E. O., Malhi, Y., Roman-Cuesta, R. M., Saatchi, S., Anderson, L. O., & Shimabukuro,  
460 Y. E. (2007). Spatial patterns and fire response of recent Amazonian droughts. *Geophysical  
461 Research Letters*, 34(7).
- 462 Aragão, L. E. O. C., Malhi, Y., Metcalfe, D. B., Silva-Espejo, J. E., Jiménez, E., Navarrete, D., ...  
463 & Vásquez, R. (2009). Above-and below-ground net primary productivity across ten  
464 Amazonian forests on contrasting soils. *Biogeosciences*, 6(12), 2759-2778.
- 465 Araújo, I., Marimon, B. S., Scalon, M. C., Cruz, W. J., Fauset, S., Vieira, T. C., ... & Gloor, M. U.  
466 (2021b). Intraspecific variation in leaf traits facilitates the occurrence of trees at the  
467 Amazonia–Cerrado transition. *Flora*, 279, 151829.
- 468 Araújo, I., Marimon, B. S., Scalon, M. C., Fauset, S., Junior, B. H. M., Tiwari, R., ... & Gloor, M.  
469 U. (2021a). Trees at the Amazonia-Cerrado transition are approaching high temperature  
470 thresholds. *Environmental Research Letters*, 16(3), 034047.
- 471 Araújo, I., Scalon, M. C., Amorim, I., Menor, I. O., Cruz, W. J., Reis, S. M., ... & Marimon, B. S.  
472 (2023). Morpho-anatomical traits and leaf nutrient concentrations vary between plant  
473 communities in the Cerrado–Amazonia transition?. *Flora*, 306, 152366.
- 474 Araújo et al. (*under review*). Taller trees exhibit greater hydraulic vulnerability in southern  
475 Amazonian forests. *Environmental and Experimental Botany*.
- 476 Bennett, A. C., Rodrigues de Sousa, T., Monteagudo-Mendoza, A., Esquivel-Muelbert, A.,  
477 Morandi, P. S., Coelho de Souza, F., ... & Phillips, O. L. (2023). Sensitivity of South American  
478 tropical forests to an extreme climate anomaly. *Nature Climate Change*, 13(9), 967-974.
- 479 Brando, P. M., Nepstad, D. C., Davidson, E. A., Trumbore, S. E., Ray, D., & Camargo, P. (2008).  
480 Drought effects on litterfall, wood production and belowground carbon cycling in an Amazon  
481 forest: results of a throughfall reduction experiment. *Philosophical Transactions of the Royal  
482 Society B: Biological Sciences*, 363, 1839-1848.
- 483 Chen, J. M., & Cihlar, J. (1995). Quantifying the effect of canopy architecture on optical  
484 measurements of leaf area index using two gap size analysis methods. *IEEE transactions  
485 on geoscience and remote sensing*, 33(3), 777-787.



- 486 Covey, K., Soper, F., Pangala, S., Bernardino, A., Pagliaro, Z., Basso, L., ... & Elmore, A. (2021).  
487 Carbon and beyond: The biogeochemistry of climate in a rapidly changing Amazon. *Frontiers*  
488 *in Forests and Global Change*, 4, 11.
- 489 Doughty, C. E., Malhi, Y., Araujo-Murakami, A., Metcalfe, D. B., Silva-Espejo, J. E., Arroyo, L., ...  
490 & Ledezma, R. (2014). Allocation trade-offs dominate the response of tropical forest growth  
491 to seasonal and interannual drought. *Ecology*, 95(8), 2192-2201.
- 492 Fan, L., Wigneron, J. P., Ciais, P., Chave, J., Brandt, M., Fensholt, R., ... & Peñuelas, J. (2019).  
493 Satellite-observed pantropical carbon dynamics. *Nature plants*, 5(9), 944-951.
- 494 Feldpausch, T. R., Phillips, O. L., Brienen, R. J. W., Gloor, E., Lloyd, J., Lopez-Gonzalez, G., ...  
495 & Vos, V. A. (2016). Amazon forest response to repeated droughts. *Global Biogeochemical*  
496 *Cycles*, 30(7), 964-982.
- 497 ForestPlots.net, Blundo, C., Carilla, J., Grau, R., Malizia, A., Malizia, L., ... & De Araujo, R. O.  
498 (2021). Taking the pulse of Earth's tropical forests using networks of highly distributed plots.  
499 *Biological Conservation*, 260, 108849.
- 500 Galbraith, D., Malhi, Y., Affum-Baffoe, K., Castanho, A. D., Doughty, C. E., Fisher, R. A., ... &  
501 Lloyd, J. (2013). Residence times of woody biomass in tropical forests. *Plant Ecology &*  
502 *Diversity*, 6(1), 139-157.
- 503 Gatti, L. V., Basso, L. S., Miller, J. B., Gloor, M., Gatti Domingues, L., Cassol, H. L., ... & Neves,  
504 R. A. (2021). Amazonia as a carbon source linked to deforestation and climate change.  
505 *Nature*, 595(7867), 388-393.
- 506 Gloor, E., Wilson, C., Chipperfield, M. P., Chevallier, F., Buermann, W., Boesch, H., ... & Sullivan,  
507 M. J. (2018). Tropical land carbon cycle responses to 2015/16 El Niño as recorded by  
508 atmospheric greenhouse gas and remote sensing data. *Philosophical Transactions of the*  
509 *Royal Society B: Biological Sciences*, 373(1760), 20170302.
- 510 Gianoli, E., & González-Teuber, M. (2005). Environmental heterogeneity and population  
511 differentiation in plasticity to drought in *Convolvulus chilensis* (Convolvulaceae). *Evolutionary*  
512 *Ecology*, 19(6), 603-613.
- 513 Girardin, C. A. J., Malhi, Y., Aragao, L. E. O. C., Mamani, M., Huaraca Huasco, W., Durand, L.,  
514 ... & Whittaker, R. J. (2010). Net primary productivity allocation and cycling of carbon along  
515 a tropical forest elevational transect in the Peruvian Andes. *Global Change Biology*, 16(12),  
516 3176-3192.
- 517 Harmon, M. E., Whigham, D. F., Sexton, J., & Olmsted, I. (1995). Decomposition and mass of  
518 woody detritus in the dry tropical forests of the northeastern Yucatan Peninsula, Mexico.  
519 *Biotropica*, 305-316.
- 520 Hughes, I. G., & Hase, T. P. A. (2010). *Measurements and their uncertainties: A practical guide*  
521 *to modern error analysis*. Oxford: Oxford University Press.
- 522 Jiménez-Muñoz, J. C., Mattar, C., Barichivich, J., Santamaría-Artigas, A., Takahashi, K., Malhi,  
523 Y., ... & Van Der Schrier, G. (2016). Record-breaking warming and extreme drought in the  
524 Amazon rainforest during the course of El Niño 2015–2016. *Scientific reports*, 6(1), 1-7.



- 525 Kaewthongrach, R., Chidthaisong, A., Charuchittipan, D., Vitasse, Y., Sanwangsri, M.,  
526 Varnakovida, P., ... & LeClerc, M. Y. (2020). Impacts of a strong El Niño event on leaf  
527 phenology and carbon dioxide exchange in a secondary dry dipterocarp forest. *Agricultural  
528 and Forest Meteorology*, 287, 107945.
- 529 Liu, J., Bowman, K. W., Schimel, D. S., Parazoo, N. C., Jiang, Z., Lee, M., ... & Eldering, A. (2017).  
530 Contrasting carbon cycle responses of the tropical continents to the 2015–2016 El Niño.  
531 *Science*, 358(6360).
- 532 Luo, X., Keenan, T. F., Fisher, J. B., Jiménez-Munoz, J. C., Chen, J. M., Jiang, C., ... & Tadić, J.  
533 M. (2018). The impact of the 2015/2016 El Niño on global photosynthesis using satellite  
534 remote sensing. *Philosophical Transactions of the Royal Society B: Biological Sciences*,  
535 373(1760), 20170409.
- 536 Machado-Silva, F., Peres, L. F., Gouveia, C. M., Enrich-Prast, A., Peixoto, R. B., Pereira, J. M.,  
537 ... & Libonati, R. (2021). Drought resilience debt drives NPP decline in the Amazon Forest.  
538 *Global Biogeochemical Cycles*, 35(9), e2021GB007004.
- 539 Malhi, Y., Aragao, L. E. O., Metcalfe, D. B., Paiva, R., Quesada, C. A., Almeida, S., ... & Teixeira,  
540 L. M. (2009). Comprehensive assessment of carbon productivity, allocation and storage in  
541 three Amazonian forests. *Global Change Biology*, 15(5), 1255-1274.
- 542 Malhi, Y., Doughty, C. E., Goldsmith, G. R., Metcalfe, D. B., Girardin, C. A., Marthews, T. R., ... &  
543 Phillips, O. L. (2015). The linkages between photosynthesis, productivity, growth and  
544 biomass in lowland Amazonian forests. *Global Change Biology*, 21(6), 2283-2295.
- 545 Malhi, Y., Girardin, C. A., Goldsmith, G. R., Doughty, C. E., Salinas, N., Metcalfe, D. B., ... &  
546 Silman, M. (2017). The variation of productivity and its allocation along a tropical elevation  
547 gradient: a whole carbon budget perspective. *New Phytologist*, 214(3), 1019-1032.
- 548 Malhi, Y., Girardin, C., Metcalfe, D. B., Doughty, C. E., Aragão, L. E., Rifai, S. W., ... & Phillips,  
549 O. L. (2021). The Global Ecosystems Monitoring network: Monitoring ecosystem productivity  
550 and carbon cycling across the tropics. *Biological Conservation*, 253, 108889.
- 551 Marimon Junior, B. H., & Haridasan, M. (2005). Comparação da vegetação arbórea e  
552 características edáficas de um cerradão e um cerrado sensu stricto em áreas adjacentes  
553 sobre solo distrófico no leste de Mato Grosso, Brasil. *Acta Botanica Brasilica*, 19, 913-926.
- 554 Marimon, B. S., Lima, E. S., Duarte, T. G., Chieregatto, L. C., & Ratter, J. A. (2006). Observations  
555 on the vegetation of Northeastern Mato Grosso, Brazil. IV. An analysis of the Cerrado-  
556 Amazonian Forest ecotone. *Edinburgh Journal of Botany*, 63, 323-341.
- 557 Marimon, B. S., Marimon-Junior, B. H., Feldpausch, T. R., Oliveira-Santos, C., Mews, H. A.,  
558 Lopez-Gonzalez, G., ... & Phillips, O. L. (2014). Disequilibrium and hyperdynamic tree  
559 turnover at the forest–cerrado transition zone in southern Amazonia. *Plant Ecology &  
560 Diversity*, 7(1-2), 281-292.
- 561 Marques, E. Q., Marimon-Junior, B. H., Marimon, B. S., Matricardi, E. A., Mews, H. A., & Colli, G.  
562 R. (2020). Redefining the Cerrado–Amazonia transition: implications for conservation.  
563 *Biodiversity and conservation*, 29(5), 1501-1517.



- 564 Marthews, T. R., Riutta, T., Oliveras-Menor, I., Urrutia, R., Moore, S., Metcalfe, D., ... & Cain, R.  
565 (2014). Measuring Tropical Forest Carbon Allocation and Cycling: A RAINFOR-GEM Field  
566 Manual for Intensive Census Plots (v3.0). Global Ecosystems Monitoring Network, Oxford.
- 567 Matricardi, E. A. T., Skole, D. L., Costa, O. B., Pedlowski, M. A., Samek, J. H., & Miguel, E. P.  
568 (2020). Long-term forest degradation surpasses deforestation in the Brazilian Amazon.  
569 *Science*, 369(6509), 1378-1382.
- 570 Metcalfe, D. B., Meir, P., Aragao, L. E. O. C., Malhi, Y., Da Costa, A. C. L., Braga, A., ... & Williams,  
571 M. (2007). Factors controlling spatio-temporal variation in carbon dioxide efflux from surface  
572 litter, roots, and soil organic matter at four rain forest sites in the eastern Amazon. *Journal of*  
573 *Geophysical Research: Biogeosciences*, 112(G4).
- 574 Metcalfe, D. B., Meir, P., Aragão, L. E. O., da Costa, A. C., Braga, A. P., Gonçalves, P. H., ... &  
575 Williams, M. (2008). The effects of water availability on root growth and morphology in an  
576 Amazon rainforest. *Plant and Soil*, 311(1), 189-199.
- 577 Miller, J. B. (1967). A formula for average foliage density. *Australian Journal of Botany*, 15, 141-  
578 144.
- 579 Miranda, S. D. C., Bustamante, M., Palace, M., Hagen, S., Keller, M., & Ferreira, L. G. (2014).  
580 Regional variations in biomass distribution in Brazilian savanna woodland. *Biotropica*, 46(2),  
581 125-138.
- 582 Moore, S., Adu-Bredu, S., Duah-Gyamfi, A., Addo-Danso, S. D., Ibrahim, F., Mbou, A. T., ... &  
583 Malhi, Y. (2018). Forest biomass, productivity and carbon cycling along a rainfall gradient in  
584 West Africa. *Global change biology*, 24(2), e496-e510.
- 585 Morandi, P. S., Marimon-Junior, B. H., De Oliveira, E. A., Reis, S. M., Valadão, M. X., Forsthofer,  
586 M., ... & Marimon, B. S. (2015). Vegetation succession in the Cerrado–Amazonian forest  
587 transition zone of Mato Grosso state, Brazil. *Edinburgh Journal of Botany*, 73(1), 83-93.
- 588 Morandi, P. S., Marimon, B. S., Eisenlohr, P. V., Marimon-Junior, B. H., Oliveira-Santos, C.,  
589 Feldpausch, T. R., ... & Phillips, O. L. (2016). Patterns of tree species composition at  
590 watershed-scale in the Amazon ‘arc of deforestation’: implications for conservation.  
591 *Environmental Conservation*, 43(4), 317-326.
- 592 Neyret, M., Bentley, L. P., Oliveras, I., Marimon, B. S., Marimon-Junior, B. H., Almeida de Oliveira,  
593 E., ... & Malhi, Y. (2016). Examining variation in the leaf mass per area of dominant species  
594 across two contrasting tropical gradients in light of community assembly. *Ecology and*  
595 *evolution*, 6(16), 5674-5689.
- 596 Nobis, M., & Hunziker, U. (2005). Automatic thresholding for hemispherical canopy-photographs  
597 based on edge detection. *Agricultural and forest meteorology*, 128(3-4), 243-250.
- 598 Nogueira, D. S., Marimon, B. S., Marimon-Junior, B. H., Oliveira, E. A., Morandi, P., Reis, S. M.,  
599 ... & Phillips, O. L. (2019). Impacts of Fire on Forest Biomass Dynamics at the Southern  
600 Amazon Edge. *Environ. Conserv.* 46, 285-292.
- 601 Oliveira, B., Marimon Junior, B. H., Mews, H. A., Valadão, M. B. X., & Marimon, B. S. (2017).  
602 Unraveling the ecosystem functions in the Amazonia–Cerrado transition: evidence of  
603 hyperdynamic nutrient cycling. *Plant Ecology*, 218(2), 225-239.



- 604 Oliveras, I., & Malhi, Y. (2016). Many shades of green: the dynamic tropical forest–savannah  
605 transition zones. *Philosophical Transactions of the Royal Society B: Biological Sciences*,  
606 371(1703), 20150308.
- 607 Palmer, P. I. (2018). The role of satellite observations in understanding the impact of El Niño on  
608 the carbon cycle: current capabilities and future opportunities. *Philosophical Transactions of*  
609 *the Royal Society B: Biological Sciences*, 373(1760), 20170407.
- 610 Peixoto, K. S., Marimon-Junior, B. H., Marimon, B. S., Elias, F., de Farias, J., Freitag, R., ... &  
611 Malhi, Y. (2017). Unravelling ecosystem functions at the Amazonia–Cerrado transition: II.  
612 Carbon stocks and CO<sub>2</sub> soil efflux in cerrado forest undergoing ecological succession. *Acta*  
613 *oecologica*, 82, 23-31.
- 614 Peixoto, K. D. S., Marimon-Junior, B. H., Cavaleiro, K. A., Silva, N. A., das Neves, E. C., Freitag,  
615 R., ... & Valadao, M. B. X. (2018). Assessing the effects of rainfall reduction on litterfall and  
616 the litter layer in phytophysiologicals of the Amazonia–Cerrado transition. *Brazilian Journal*  
617 *of Botany*, 41(3), 589-600.
- 618 Phillips, O. L., Aragão, L. E., Lewis, S. L., Fisher, J. B., Lloyd, J., López-González, G., ... & Torres-  
619 Lezama, A. (2009). Drought sensitivity of the Amazon rainforest. *Science*, 323(5919), 1344-  
620 1347.
- 621 Ratter, J. A., Richards, P. W., Argent, G., & Gifford, D. R. (1973). Observations on the vegetation  
622 of northeastern Mato Grosso: I. The woody vegetation types of the Xavantina-Cachimbo  
623 Expedition area. *Philosophical Transactions of the Royal Society of London. B, Biological*  
624 *Sciences*, 266(880), 449-492.
- 625 Reis, S. M., Lenza, E., Marimon, B. S., Gomes, L., Forsthofer, M., Morandi, P. S., ... & Elias, F.  
626 (2015). Post-fire dynamics of the woody vegetation of a savanna forest (Cerradão) in the  
627 Cerrado–Amazon transition zone. *Acta Botanica Brasílica*, 29, 408-416.
- 628 Reis, S. M., de Oliveira, E. A., Elias, F., Gomes, L., Morandi, P. S., Marimon, B. S., ... & Lenza,  
629 E. (2017). Resistance to fire and the resilience of the woody vegetation of the “Cerradão” in  
630 the “Cerrado”–Amazon transition zone. *Brazilian Journal of Botany*, 40(1), 193-201.
- 631 Reis, S. M., Marimon, B. S., Marimon Junior, B. H., Morandi, P. S., Oliveira, E. A. D., Elias, F., ...  
632 & Phillips, O. L. (2018). Climate and fragmentation affect forest structure at the southern  
633 border of Amazonia. *Plant Ecology & Diversity*, 11(1), 13-25.
- 634 Reis, S. M., Marimon, B. S., Esquivel-Muelbert, A., Marimon Jr, B. H., Morandi, P. S., Elias, F., ...  
635 & Phillips, O. L. (2022). Climate and crown damage drive tree mortality in southern  
636 Amazonian edge forests. *Journal of Ecology*, 110(4), 876-888.
- 637 Reis, S. (2023). Savanna is more resistant and resilient to tropical drought than transitional forest.  
638 Dryad Dataset: <https://doi.org/10.5061/dryad.rjdfn2zhw>
- 639 Rezende, A. V., Vale, A. D., Sanquetta, C. R., Figueiredo Filho, A., & Felfili, J. M. (2006).  
640 Comparação de modelos matemáticos para estimativa do volume, biomassa e estoque de  
641 carbono da vegetação lenhosa de um cerrado sensu stricto em Brasília, DF. *Scientia*  
642 *Forestalis*, 71(2), 65-73.



- 643 Ribeiro, J. F., Walter, B. M. T. (2008). As principais fitofisionomias do bioma Cerrado. *Cerrado*  
644 *Ecologia e Fauna*. Brasília: Embrapa Informação Tecnológica 1, 153 – 221.
- 645 Rifai, S. W., Girardin, C. A., Berenguer, E., del Aguila-Pasquel, J., Dahlsjö, C. A., Doughty, C. E.,  
646 ... & Malhi, Y. (2018). ENSO Drives interannual variation of forest woody growth across the  
647 tropics. *Philosophical Transactions of the Royal Society B: Biological Sciences*, 373(1760),  
648 20170410.
- 649 Riutta, T., Malhi, Y., Kho, L. K., Marthews, T. R., Huaraca Huasco, W., Khoo, M., ... & Ewers, R.  
650 M. (2018). Logging disturbance shifts net primary productivity and its allocation in Bornean  
651 tropical forests. *Global Change Biology*, 24(7), 2913-2928.
- 652 Schleppi, P., Conedera, M., Sedivy, I., & Thimonier, A. (2007). Correcting non-linearity and slope  
653 effects in the estimation of the leaf area index of forests from hemispherical photographs.  
654 *Agricultural and Forest Meteorology*, 144(3-4), 236-242.
- 655 Silvério, D. V., Brando, P. M., Bustamante, M. M., Putz, F. E., Marra, D. M., Levick, S. R., &  
656 Trumbore, S. E. (2019). Fire, fragmentation, and windstorms: A recipe for tropical forest  
657 degradation. *Journal of Ecology*, 107(2), 656-667.
- 658 Soares Jancoski, H., Schwantes Marimon, B., C. Scalon, M., de V. Barros, F., Marimon-Junior,  
659 B. H., Carvalho, E., ... & Oliveras Menor, I. (2022). Distinct leaf water potential regulation of  
660 tree species and vegetation types across the Cerrado–Amazonia transition. *Biotropica*,  
661 54(2), 431-443.
- 662
- 663
- 664
- 665
- 666
- 667
- 668
- 669
- 670
- 671
- 672
- 673
- 674